# ANALYSIS OF FREEZE-FRACTURE ELECTRON MICROGRAPHS BY A COMPUTER-BASED TECHNIQUE

ROLF J. MEHLHORN *and* LESTER PACKER

*From the Membrane Bioenergetics Group, Energy and Environment Division, Lawrence Berkeley Laboratory, and the Department of Physiology-Anatomy, University of California, Berkeley, California 94720*

ABSTRACT A procedure is described for deriving a numerical characterization of membrane particle patterns revealed in freeze-fracture electron micrographs. Rectangular coordinates of the particles are obtained with high precision by means of an electronic digitizing device. These coordinates are fed into a large computer and analyzed in terms of (*a*) a local particle density function in terms of variable subdivisions of the membrane, and (*b*) an interparticle distance function describing all particle pairs within the membrane. It is found that the particle density function gives the most useful description of clustering provided that particle-free patches are monitored along with nonvanishing particle densities. Theoretical particle patterns are generated with the computer by means of a random number generator to provide defined aggregation states which serve as standards of comparison for observed particle patterns.

## INTRODUCTION

The freeze-fracture technique of electron microscopy provides a high resolution view of biological membranes—usually of the hydrophobic interior, although, upon etching, surface structures are revealed (1). The hydrophobic membrane interior is studded with particles, presumed to be protein, or lipoprotein, of a range of diameters. These particles usually seem to be randomly arranged but occasionally they are observed to be clustered under defined physiological conditions. More subtle clustering of membrane particles may be a general phenomenon but would probably have escaped detection by subjective criteria.

The nature of these membrane particle patterns has been used to a limited extent to identify different intracellular membranes (2–4), and has been correlated with cellular environments and physiological states (5, 6). An example of a human fibroblast cell as revealed by the freeze-fracture technique is shown in Fig. 1. Subcellular membranes are readily distinguished from each other on the basis of their membrane particle patterns. Quite likely, a quantitative analysis of particle patterns would be a valuable tool for the identification of normal and aberrant membrane states. We have, therefore, undertaken to characterize freeze-fracture particle patterns quantitatively with the aid

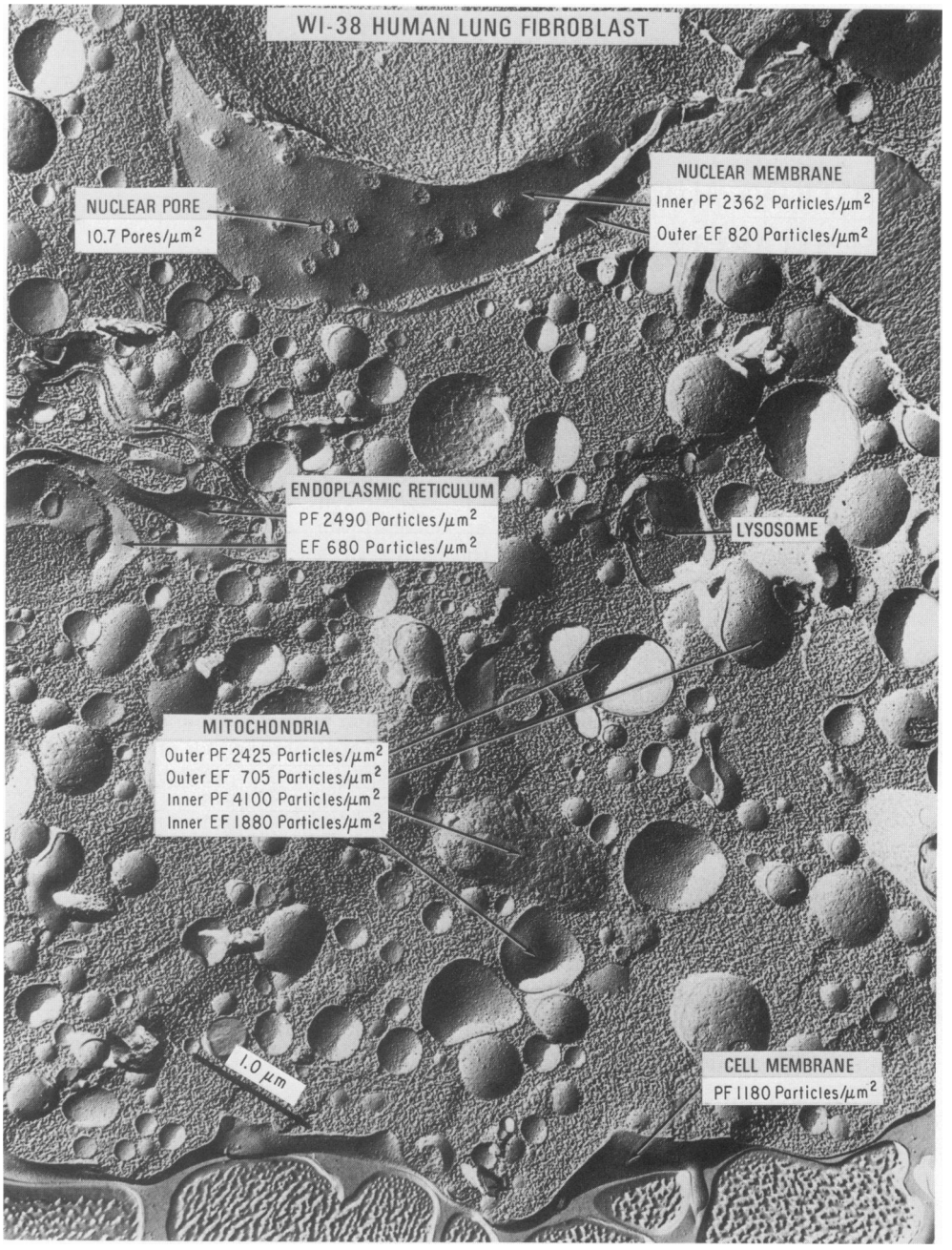


FIGURE 1 An example of a freeze-fracture mammalian cell, illustrating the variety of membrane particle patterns arising from the different membranes. Particle densities per square micrometer are given for several of the split membranes. Fracture faces are identified in terms of simplified terminology proposed in a recent publication (9).

of a computer analysis and semiautomated scanning techniques of electron micrographs.

## THEORY

A number of options are available for obtaining a mathematical description of a pattern of point particles (7). Such generalized schemes do not readily lend themselves to the analysis of freeze-fracture patterns however, for two reasons: (*a*) the membrane area is usually quite limited, often containing only a small number of particles, and (*b*) the finite particle size represents a marked departure from the ideal of a point particle pattern. Hence, any analytical scheme must contend with the problem of the finite size of the membrane segment seen in the electron micrograph, and it must also deal with likelihood of particle crowding, which would limit the minimum separation of particles. Two approaches were investigated for providing a concise parametric description of particle patterns. In the first, an interparticle distance function was generated for all particle pairs in a rectangular segment of the membrane. This was compared with a theoretical distance function depending on the particle diameter distribution and the dimensions of the rectangular area. By fitting the observed curve to the theoretical one at small distances, it was possible to derive information about the particle diameter distribution. Departures of the observed curve from the theoretical curve represent a measure of particle clustering. Unfortunately, this treatment proved to be highly consuming of computer time and, in fact, proved to be of limited utility for the identification of patterns that were readily judged to be nonrandom by visual criteria. As will be discussed later, this was due, in part, to a neglect of the particle-free "smooth" areas of the picture. Therefore, this analytical approach was discarded in favor of a more efficient and less rigorous numerical procedure.

The numerical procedure that proved to be most convenient and efficient for the analysis of particle patterns basically consists of a simple counting procedure of particles within square subdivisions of the picture area. With this procedure particle frequency histograms are generated as a function of the number of particles per subdivision area.

More precisely, a square picture area is subdivided into a $(2.5 \times M \times M)^{1/2}$ grid and particles are counted within each of the square subdivisions of unit area. Multiples of this square area of dimension $N \times N$ are also considered. If the number of particles is denoted by $I$, then the frequency histograms are given by the functions

$$F_N(I) = \sum_{i=j}^{50} \sum_{j=1}^{50} u\left(\sum_{k=i}^{i+N} \sum_{l=j}^{j+N} C_{kl} - I\right),$$

where $C_{kl}$ is the number of particles within the $(k, l)$ subdivision of the picture area, and where the unit function $u(x)$ is unity for $x = 0$ and vanishes otherwise. Generally, $N$ varies from 1 to 8.

An important feature of this approach is that empty areas, corresponding to $I = 0$ are also considered. Three special cases can be considered to clarify the significance

of these histograms: (*a*) uniform particle distribution—in this case $F_N(I)$ would vanish everywhere except for $I = M \times M \times N \times N/2500$, since the density of particles is the same everywhere; (*b*) random particle distribution—in this case, for sufficiently small areas $N \times N$, the particle density would vary over the picture area and the histograms $F_N(I)$ would have some characteristic width ranging from $I = 0$ upwards through the maximum local particle density; and (*c*) a simple clustering model corresponding to all the particles uniformly clustered into half of the picture area—in this case $F_N(I)$ would be nonvanishing for $I = 0$ and for $I = M \times M \times N \times N/1250$. Thus, it may be stated that the overall width of the histograms provide a measure of the particle distribution. Indeed, if the widths for a random particle distribution were known, then the widths of the observed histograms would immediately serve to identify relatively uniform or clustered patterns.

## DATA REDUCTION

Particle identification is carried out visually. Many of the particles are at the margin of detection because of size and contrast variations within the replica. Therefore, fully automatic data reduction was rejected in favor of a semiautomatic approach in which a trained observer identified particles within a designated area of the membrane.

Conversion of the particle positions in the membrane to Euclidean coordinates is achieved by means of a scanning machine originally designed for the data reduction of bubble chamber films at the Lawrence Berkeley Laboratory. A 10-fold enlarged image of the electron micrograph is projected on a table and particles are manually pinpointed with a two-dimensional digitizing device having a resolution on the table of 0.0125 cm. Whenever a particle has been pinpointed a foot pedal is pressed to record the digitized information on magnetic tape. This tape can be fed subsequently into a computer for mathematical analysis.

A serious difficulty with this approach is that the membrane area is generally not coplanar with the replica owing to the curvature of the membrane and to the erratic development of the fracture plane during freeze cleaving. Thus particle coordinates will generally be foreshortened in some direction. There is no straightforward technique for the correction of this error; instead an analytical technique must be devised which is largely independent of picture tilt.

It should be noted that the highly sophisticated scanning machine used for data reduction is not crucial for the subsequent histogram analysis, and reasonably accurate particle coordinates can be obtained, albeit more laboriously, by means of direct measurements on a photographic enlargement of a membrane segment.

## RESULTS

### *An Example of the Reduction of a Clustered Particle Pattern*

An example of the conversion of an electron micrograph to computer coordinates is shown in Fig. 2. The distortion of the latter is due to the low resolution of the line printer used to present an image of the digitized data and is not a true reflection of the

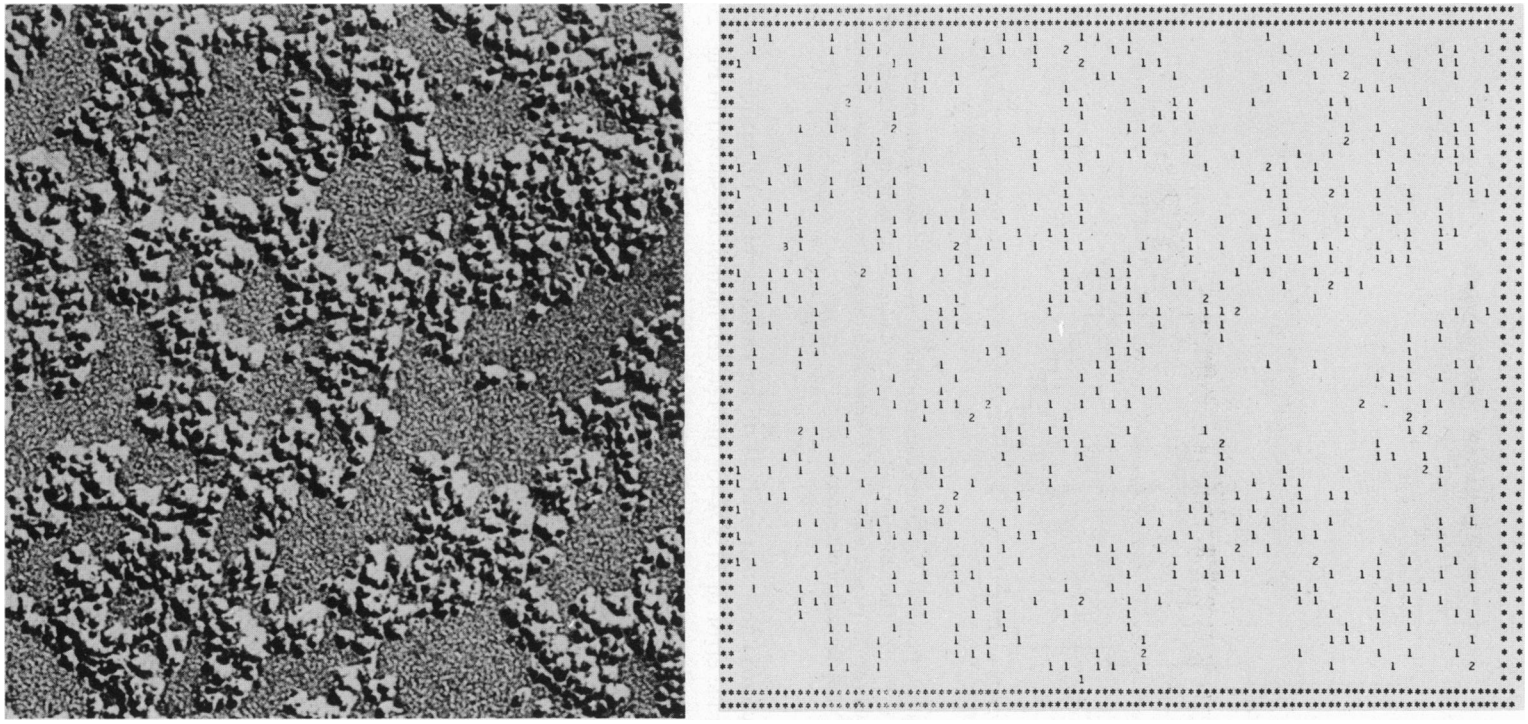

FIGURE 2 An example of an electron micrograph of a freeze-fractured human red blood cell and the corresponding computer printout of the digitized particle coordinates.

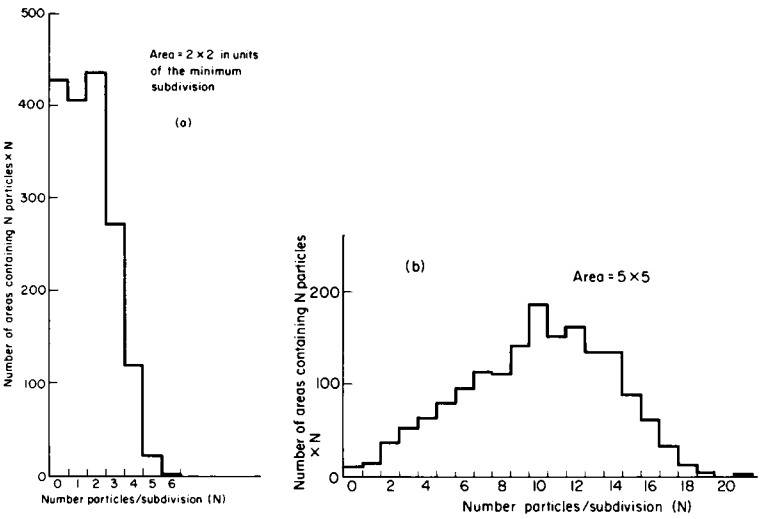


FIGURE 3 Particle frequency histograms corresponding to two partitions of the electron micrograph shown in Fig. 2. The minimum cell size was a square of dimension $u = E/40$ where $E$ is the dimension of the picture edge. (*a*) Counts were carried out within cells of dimension $2u \times 2u$. (*b*) Counts for cells of dimension $5u \times 5u$.

accuracy of the coordinates. An analysis of the reproducibility of particle coordinates revealed an average error of 21.5 Å for the red cell membrane shown in Fig. 2. This error can be reduced considerably by using plates of higher magnification, of course.

The reduction of the digitized data to particle frequency histograms is illustrated in Fig. 3. These correspond to particle counts carried out within two of the eight mesh sizes superimposed over the picture area. It is generally observed that the frequency functions $F(I)$ are roughly bell shaped and hence can be characterized in terms of their mean positions $\langle I \rangle$ and their widths, given by the second moments

$$S_N = \left( \sum_{I=1}^{60} (I - \langle I \rangle)^2 F(I) \Big/ \left[ N^2 \times \sum_{I=1}^{60} F(I) \right] \right)^{1/2}.$$

As was indicated earlier, the second moments, $S_N$, of the particle frequency histograms provide a measure of the degree of clustering. By generating histograms for a variety of mesh sizes it is possible to determine characteristic areas for which departures from randomness are a maximum. Accordingly, second moments are generated for a range of mesh sizes as shown in Fig. 4. A comparison of these with second moment values determined from random patterns leads to a characterization of clustering.

A distance function $G(r)$ corresponding to the particle density as a function of interparticle distance was generated for all particle pairs and is shown in Fig. 5. This is compared with a theoretical function for a random particle pattern which takes into account the particle size distribution (assuming a mean diameter of 40 Å) and the reduction of $G(r)$ as $r$ approaches the dimensions of the picture area (see Appendix).

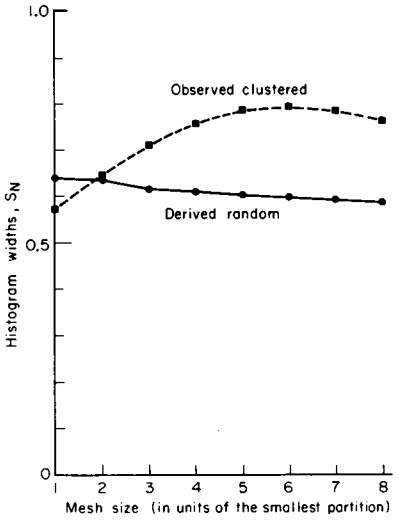


FIGURE 4

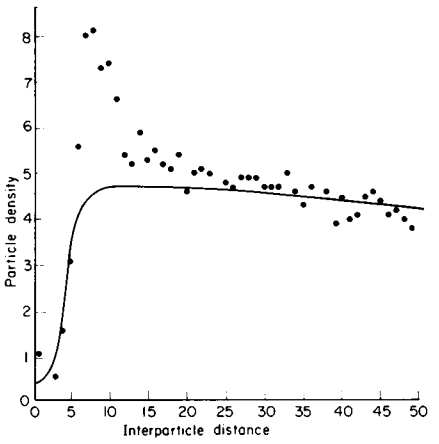


FIGURE 5

FIGURE 4 Variation of the widths of the histograms as a function of the cell size for which particle counts were conducted. The cell size varied from $1u$ to $8u$ where $u$ was defined as in Fig. 3. (_____) Computer-generated random array of point particles, (———) observed particle pattern shown in Fig. 1.

FIGURE 5 Distance function corresponding to the particle pattern of Fig. 2. A theoretical function describing a random array of particles of mean diameter 40 Å is presented as well (solid line). One ordinate unit correspond to 1,500 particles/$\mu m^2$ while one abscissa unit corresponds to 10.6 Å.

Note that the two curves merge at distances of the order of 200 Å, i.e. distances considerably smaller than the visually observed particle patches.

To study reproducibility of the derived aggregation parameters two questions were examined: (*1*) what is the variation in these parameters with different observers using individual criteria for particle identification, and (*2*) are these parameters reproducible for two different areas selected from the same membranes?

The results of an analysis of several subdivisions of a single red cell membrane involving three different observers are given in Table I. The second moment values given in this table refer to $S_N - \bar{S}_N$ where $\bar{S}_N$ are values of the histogram widths derived from computer-generated random particle patterns as described in the next section.

### *Computer-generated Particle Patterns*

A CDC 7600 computer was used to generate a random pattern using a random number function to produce alternately values of $x$ and $y$ within the picture area. The second moment curve arising from an analysis of random patterns is shown in Fig. 4 also. This curve gives the values of $\bar{S}_N$, i.e. it represents the weighted average of second moments derived from nine computer-generated random patterns. Of course, the fluctuations of the second moment curves diminish as the number of particles within a

TABLE I

VARIATION OF THE DERIVED PARAMETERS WITH AREA SELECTION AND OBSERVER

Histogram widths, relative to theoretical random pattern values, as a function of partition size. Units are described in the legend to Fig. 4 and in the text.

| | Number of particles | 1 | 2 | 3 | 4 | 5 | 6 | 7 | 8 | Sum |
|---|---|---|---|---|---|---|---|---|---|---|
| OBSERVER I | | | | | | | | | | |
| Area 1 | 639 | −0.0681 | 0.0085 | 0.0934 | 0.1472 | 0.1823 | 0.1962 | 0.1921 | 0.1790 | 0.9306 |
| Area 2 | 672 | −0.0246 | 0.0467 | 0.1071 | 0.1398 | 0.1570 | 0.1652 | 0.1592 | 0.1678 | 0.9182 |
| Area 3 | 608 | −0.0428 | 0.0467 | 0.1099 | 0.1455 | 0.1839 | 0.2034 | 0.2211 | 0.2446 | 1.1123 |
| OBSERVER II | | | | | | | | | | |
| Area 2 | 940 | −0.0272 | 0.0839 | 0.2053 | 0.2699 | 0.3137 | 0.3428 | 0.3743 | 0.3949 | 1.7128 |
| OBSERVER III | | | | | | | | | | |
| Area 1 | 559 | −0.0374 | 0.0513 | 0.1117 | 0.1544 | 0.1682 | 0.1598 | 0.1478 | 0.1171 | 0.8729 |

TABLE II

STATISTICAL NOISE IN THE DERIVED PARAMETERS

Histogram widths of theoretical patterns relative to mean values as a function of partition size. Values for a pattern tilted 30° from normal are given in the last row (see text).

| Number of particles | 1 | 2 | 3 | 4 | 5 | 6 | 7 | 8 | Sum |
|---|---|---|---|---|---|---|---|---|---|
| 800 | 0.006 | 0.006 | 0.008 | −0.002 | −0.004 | −0.004 | −0.004 | 0.008 | 0.023 |
| 800 | 0.001 | −0.004 | −0.017 | −0.024 | −0.024 | −0.026 | −0.021 | −0.018 | −0.132 |
| 800 | 0.010 | 0.029 | 0.032 | 0.015 | 0.018 | 0.016 | 0.015 | 0.013 | 0.148 |
| 600 | −0.002 | −0.020 | −0.025 | −0.016 | −0.021 | −0.015 | −0.013 | −0.004 | −0.116 |
| 600 | −0.028 | −0.047 | −0.069 | −0.069 | −0.075 | −0.076 | −0.080 | −0.074 | −0.519 |
| 600 | −0.015 | 0.004 | 0.012 | 0.021 | 0.016 | 0.016 | 0.022 | 0.033 | 0.112 |
| 400 | 0.021 | 0.020 | 0.042 | 0.055 | 0.071 | 0.075 | 0.077 | 0.082 | 0.442 |
| 400 | 0.007 | 0.003 | 0.003 | 0.001 | −0.001 | 0.002 | −0.006 | −0.037 | −0.030 |
| 400 | 0.006 | 0.010 | 0.031 | 0.064 | 0.068 | 0.059 | 0.040 | 0.005 | 0.294 |
| 800/30° | −0.005 | −0.021 | −0.035 | −0.033 | −0.033 | −0.026 | −0.003 | −0.014 | −0.140 |

picture area increases. This is shown in Table II where these fluctuations are tabulated as a function of the particle number.

A pattern corresponding to particle aggregation was also generated. In this model 70% of the particles were caused to be aggregated within clusters of maximum diameter of 2% of the picture edge. The distribution of particle numbers in these clusters was a random function uniform in the range from 2 to 4. The resulting pattern is shown in Fig. 6.

In an effort to reproduce observed patterns having a high degree of particle clustering another nonrandom pattern was generated by the computer. In this approach rectangular particle-free patches were first generated until 30% of the picture area was accounted for. These patches had dimensions in the range of 10–15% of the picture edge. Then particles were produced just as in the random case, but were not accepted by the computer if they fell into one of the void patches. The resulting particle pattern is shown in Fig. 7. It should be noted here that the void patches did not match the observed pattern well if they were centered at random positions within the picture area. Instead they had to be dispersed so as to reduce overlap of the patches.

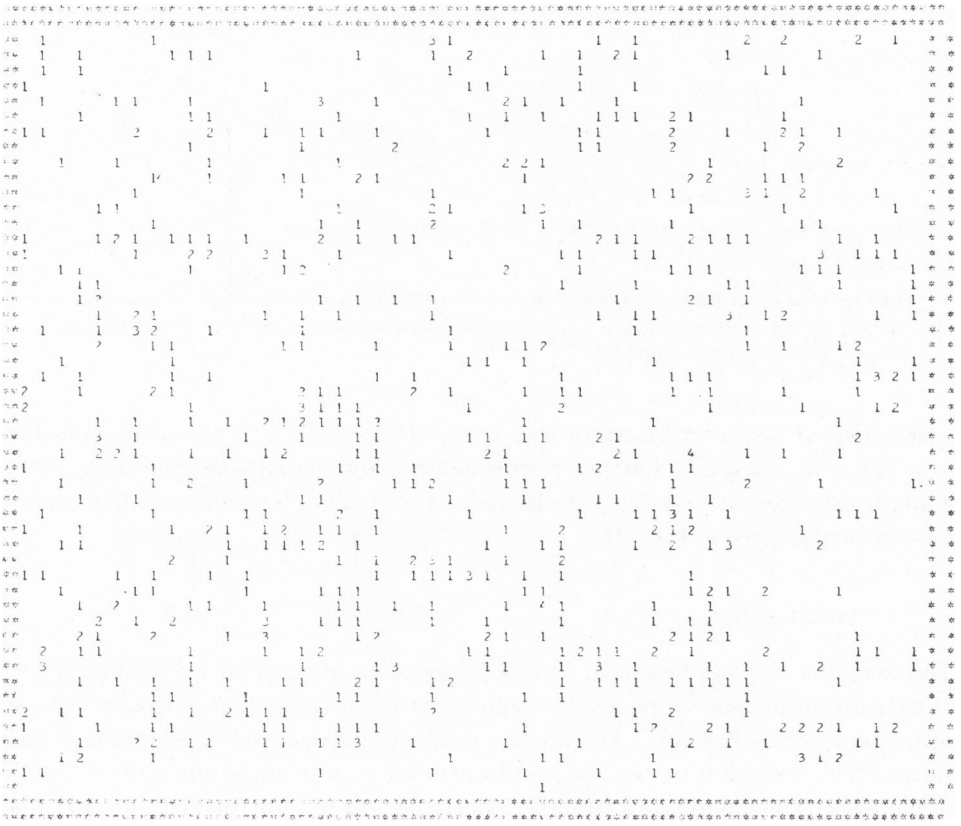

FIGURE 6 Computer-generated pattern with a provision for particle clustering. 70% of the particles were caused to cluster in sets of two to four without domains of about 80 Å in diameter.

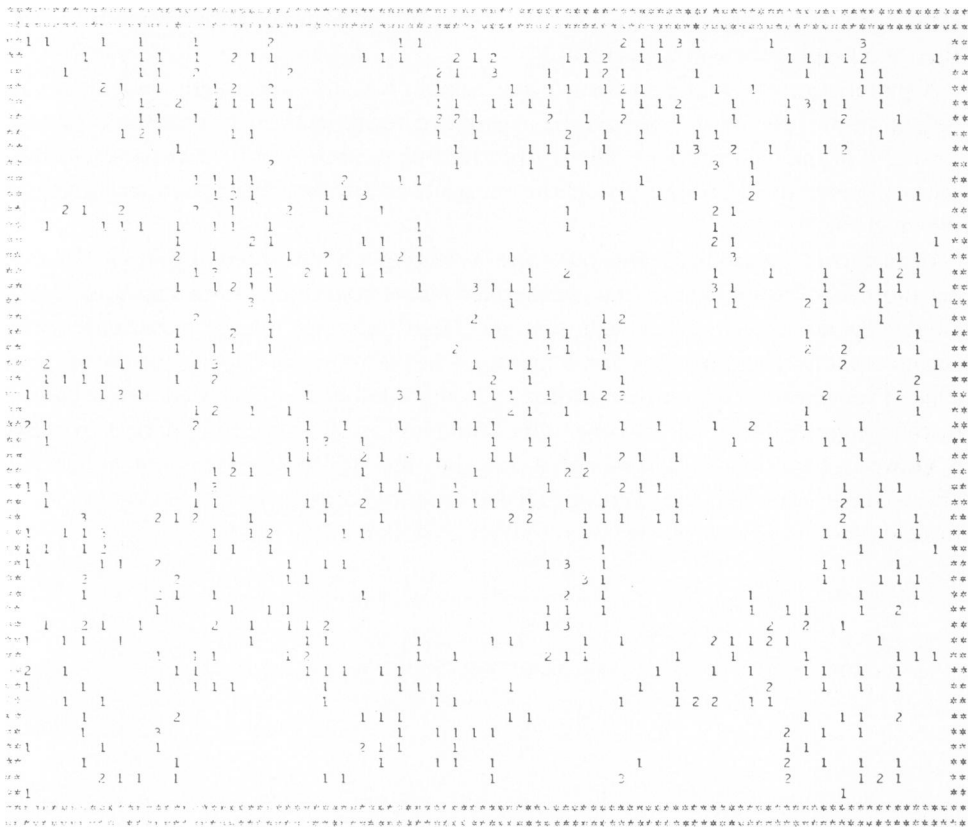

FIGURE 7 Computer-generated pattern with provisions for particle-free areas. About 30% of the total picture area was devoted to rectangular particle-free patches having dimensions in the range of 10–15% of the picture edge.

The effect of local membrane tilt with respect to the replica plane was examined by imposing a 30° angle on a computer-generated random particle pattern and selecting a square area from the resulting projection. The results of an analysis of the tilted pattern are displayed in Table II.

## DISCUSSION

The computer analysis described in this paper is an attempt to establish objective criteria for the analysis of relatively simple electron micrographs, i.e. freeze-fractured membrane particle patterns. Despite the relatively uncomplicated morphology considered here, it was not possible to avoid subjective factors in the initial identification of particles. Two approaches towards data reduction were considered: (*a*) an interparticle distance function and (*b*) a local particle density analysis as a function of varying square domain sizes. For both methods reference functions defining random

particle patterns were established and the observed patterns were analyzed relative to these.

One difficulty with the local density analysis is that the reference function for a random particle distribution fails to take into account the finite particle size. As a result the observed patterns which seem to be random by visual criteria are all displaced with respect to the reference function. This is to be expected on the basis of the following argument: If the particle sizes were all equal and large enough to put all the particles into contact then the particle distribution would be uniform and the second moments would vanish. Thus, it is plausible that an increase in particle sizes for a fixed pattern in general would reduce the values of the second moments, $S_N$. Of course, the reference function was generated for a point particle array, i.e. there was no restriction placed on the minimum particle separation. This was necessary for two reasons: (*a*) the desirability of having a single reference function which could be established once and for all, and (*b*) the difficult and time consuming task of taking finite particle diameters into account when generating random patterns with the computer.

The generation of the local density function over all the mesh subdivisions and for various domain sizes is highly time consuming. For the larger domain sizes there is a great deal of redundancy, i.e. a given particle is counted many times in order to reduce the statistical noise in the particle frequency histograms. However, it is important to obtain histograms which are smooth and noise free in order to derive meaningful second moments and hence clustering information. The amount of computing required to achieve this end is considerable; therefore an electronic computer is indispensable for the analysis.

The distance function calculation gives useful information about the nearest neighbor distances of closely spaced particle pairs. From this information the particle diameters can be inferred. These are considerably smaller than those obtained from direct diameter measurements. This is to be expected since the thickness of the platinum shadowing film would contribute to the latter but not to the center to center distances of particles. Of course, only a few particle pairs contribute to the interparticle function at small distances. This, as well as the inaccuracies in the particle positions, limit the reliability of the inferred mean particle diameters.

### *Computer-generated Particle Patterns*

In order to achieve correlation of the derived parameters and the actual degree of clustering, the computer was used to generate random patterns as well as defined clustering of particles and particle-free areas. In addition the effect of membrane tilt with respect to the fracture plane was considered.

It was found that observed patterns in which particle patches were readily discerned could be correlated with computer patterns in which particle-free areas were stipulated but not with patterns in which the particles were caused to aggregate. If the smooth areas are identified as lipid and the particle as protein or lipoprotein aggregates this could be interpreted as lipid crystallization which would lead to particle crowding on the periphery of the lipid "crystals." This result appears to differ from the finding of

Finegold who asserts that a dynamic computer model of particle diffusion allowing for close range interaction between particles simulates observed membrane aggregation stages (8).

Computer-generated random patterns were used to estimate the extent of statistical noise in the derived parameters expected for a given number of particles. While this approach is considerably more convenient and efficient than the use of observed particle patterns, the neglect of the particle sizes in the random computer patterns leads to an overestimation of the statistical noise. This can be understood by considering that the area occupied by the particles is often a considerable proportion of the total and this reduces the variability.

The effect of a membrane tilt seems to be negligible for a random pattern. Of course, tilt would reduce the area of patches by a factor of $1-\cos\theta$, where $\theta$ is the angle between the membrane surface and the fracture plane. Hence, it is to be expected that the variability of clustering parameters due to tilt would increase with the degree of patchiness. However, this is compensated by the fact that large departures from randomness are more easily identified.

### *Computer Analyses vs. Visual Criteria of Clustering*

Our experience with the analysis of particle patterns with a computer indicates that visual criteria and computer techniques described here are of comparable sensitivity for cluster identification. Indeed, marginal clustering seems to be more readily recognized by a human observer. Thus the principal virtue of the computer technique appears to be reproducibility and quantitation. Improvements in the computer technique would be realized if the particle frequency histograms were not confined to counts for square areas. The human eye is not limited in this regard; it has no difficulty in following a complicated patch boundary. On the other hand, the computer time required to follow such boundaries is too great to make such an approach feasible at the present time.

The authors would like to acknowledge the collaboration of Dr. Daniel Branton and Dr. E. Elgsaeter in the initial stages of this investigation, and for making available replicas of freeze-fracture electron micrographs.

This research was supported by the Muscular Dystrophy Association of America and the Energy Research and Development Administration.

*Received for publication 2 October 1975.*

## REFERENCES

1. BRANTON, D., and D. W. DEAMER. 1972. Membrane structure. *Protoplasmalogia.* **II/E/1**:1.
2. WRIGGLESWORTH, J. M., L. PACKER, and D. BRANTON. 1970. Organization of mitochondrial structure as revealed by freeze-etching. *Biochim. Biophys. Acta.* **205**:125.
3. MELNICK, R. L., and L. PACKER. 1971. Freeze-fracture faces of inner and outer membranes of mitochondria. *Biochim. Biophys. Acta.* **253**:503.
4. PACKER, L., C. W. MEHARD, G. MEISSNER, W. L. ZAHLER, and S. FLEISCHER. The structural role of lipids in mitochondrial and sarcoplasmic reticulum membranes—Freeze-fracture electron microscopy studies. *Biochim. Biophys. Acta.* **363**:159.

5. OJAKIAN, G. K., and P. SATIR. 1974. Particle movements in chloroplast membranes: quantitative measurements of membrane fluidity by the freeze fracture technique. *Proc. Natl. Acad. Sci. U.S.A.* **71:** 2052.
6. TORRES-PEREIRA, J., R. MEHLHORN, A. D. KEITH, and L. PACKER. 1974. Changes in membrane lipid structure of illuminated chloroplasts. Studies with spin-labeled and freeze-fractured membranes. *Arch. Biochem. Biophys.* **160:**350.
7. YOUNG, T. Y., and T. W. CALVERT. 1974. Classification, Estimation and Pattern Recognition. American Elsevier Publishing Co., New York.
8. FINEGOLD, L. X. 1975. Cell membranes fluidity: molecular modeling of particle aggregation. Programme of the 5th International Biophysics Congress, Bella Centret. Copenhagen. Abstr. P-340.
9. BRANTON, D., S. BULLIVANT, N. B. GILULA, M. J. KARNOVSKY, H. MOOR, K. MÜHLETHALER, D. H. NORTHCOTE, L. PACKER, B. SATIR, P. SATIR, V. SPETH, L. A. STAEHLIN, R. L. STEERE, and R. S. WEINSTEIN. 1975. Freeze-etching nomenclature. *Science (Wash. D.C.).* **190:**54.

## APPENDIX

(*A*) For a continuous distribution of particles the interparticle density function within an area in the range $0 \leq x \leq l$ and $0 \leq y \leq l$ is given by $\rho(r) = \int_0^l dx_1 \int_{x_1}^l dx_2 \int_0^l dy_1 \int_{y_1}^l dy_2$ $\delta(|\mathbf{r}_1 - \mathbf{r}_2| - r)$ where $\int_{x_1}^{x_2} \delta(x)\delta x = l$ if $x_1 \leq x \leq x_2$. The solution of this integral equation yields:

$$\begin{aligned}\rho(r) &= r^2(l - \tfrac{1}{2}\sqrt{r^2 - l^2})[1 + \sin^{-1}(\sqrt{r^2 - l^2}/r)] \\ &\quad - \tfrac{1}{2}lr^2 \sin^{-1}(l/r) - l^2\sqrt{r^2 - l^2} \\ &\quad - \tfrac{1}{6}[l^3 - (r^2 - l^2)^{3/2}] \text{ for } r > l; \\ &= l^2 r - [\tfrac{1}{2} + (\pi/4)]lr^2 + \tfrac{1}{3}r^3 \text{ for } r < l.\end{aligned}$$

(*B*) The transformation from an array of infinitesimal particles to an array of particles of diameter $D$ is given by

$$\rho(r') = \int_o^D \int_o^{2\pi} d\theta dr \rho(r)\,\delta(r' - f(r)) + \int_D^\infty \int_{-\theta'}^{\theta'} d\theta dr \rho(r)\,\delta(r' - f(r)),$$

assuming that particles described by $\rho(r)$ when $r < D$ are displaced to some point $r > D$ by an elastic collision at $r = D$, and integrating over all scattering angles. A similar function for which the diameter of two colliding particles differ subject to $r_1 + r_2 = D$, where $r_1$ and $r_2$ are the radii of the two particles was solved numerically with the computer and gave the surprisingly simple result

$$\rho(r') = o\, r' < D, \rho(\infty)\, r' \geq D.$$

(*C*) If the set of minimum interparticle distances is assumed to be given by a Lorentzian distribution $f(D) = 1/[a^2 + (D - D_o)^2]$, then we have the result $\rho(r') = \rho(\infty)(\frac{1}{2} + [1/\pi] \tan^{-1}$ $[(r' - D_o)/a])$. This function was multiplied by the function given in part A and normalized to the proper asymptotic particle density to give the theoretical interparticle distance function.